JOURNAL OF GUIDANCE, CONTROL, AND DYNAMICS
Vol. 29, No. 2, March–April 2006

Generalized Vector Explicit Guidance

Ernest J. Ohlmeyer* and Craig A. Phillips†
Naval Surface Warfare Center, Dahlgren, Virginia 22448

This paper proposes and evaluates a new guidance law termed generalized vector explicit guidance (GENEX). This guidance law can simultaneously achieve design specifications on miss distance and final missile–target relative orientation. The latter may be used to enhance the performance of warheads the effectiveness of which is influenced by the terminal encounter geometry. The GENEX guidance law is parameterized in terms of a design coefficient that determines the degree of curvature in the trajectory. Feasibility of GENEX guidance was demonstrated by its application to two weapon scenarios. The first was an air-to-air missile terminal homing scenario. Assuming ideal sensor information and a single-lag missile response model, the guidance was shown to perform well against an air target performing evasive maneuvers. A specified zero-aspect terminal encounter angle was achieved while simultaneously minimizing miss distance. The second application involved an air-to-surface munition released from an unmanned air vehicle. The GENEX guidance law was able to produce trajectories satisfying a terminal impact angle constraint. In addition, an engagement region of sufficient size was shown to be achievable using guidance gains scheduled with target location and weapon release altitude.

I. Introduction

THE increasing severity of airborne threats against U.S. Navy ships has placed new and challenging demands on defensive missile systems. Threat missiles and aircraft can perform high-speed, rapid maneuvers over widely varying flight regimes, thereby taxing the response of interceptor guidance and control systems. To cope, interceptor missiles must have increased maneuverability and faster time constants. In addition, the payloads carried by these evolving threats are being increasingly hardened. As a result, interceptor warheads must be placed accurately on or very near the target body for assured destruction.

In addition, delivery of precision-guided munitions against surface targets is complicated by the need to maximize the effectiveness of the warhead and the survivability of the launch vehicle. The former requirement places constraints on the final flight path angles at intercept to ensure warhead effectiveness. The latter requirement drives the selection of the launch vehicle cruise altitude. The launch altitude, the launch vehicle sensor characteristics, and the maneuverability limits, in turn, place constraints on the munition trajectory design. Improved guidance is required to shape the trajectory effectively to satisfy all these operational requirements.

The effectiveness of many warhead systems is a strong function of the miss distance and the relative approach angle between target and missile. For example, in an air-to-air scenario, a fragmentation warhead initiated by a fuzing mechanism is less sensitive to fuze timing errors when the longitudinal axis of the warhead is roughly parallel to the target body. This is because the available window of opportunity for the fragments to intersect the target is increased during a head-on encounter. Alternatively, many surface targets are more vulnerable from a topside aspect, motivating a desire to attack them from a near-vertical orientation to maximize terminal lethality.

To optimize the terminal engagement geometry and maximize warhead effectiveness, guidance laws can be designed that reduce the miss distance to a small value while simultaneously achieving a specified final orientation relative to the target. An example of such a law is *explicit guidance* (sometimes called *E-guidance*), which attempts to maneuver a weapon from its current position to a desired final position while controlling the orientation of the final velocity vector. The original version of explicit guidance is due to G. Cherry[1] and is further explored in Refs. 2 and 3. Other guidance methods that attempt to control both miss distance and terminal geometry have been proposed in Refs. 4–12.

It is possible to derive a generalized form of explicit guidance (see Ref. 10) in which the cost function to be minimized is itself specified in terms of a user-defined parameter. This parameter, along with the initial and final flight-path angles, becomes a design parameter that the user may adjust to achieve particular performance objectives. The generalized form of explicit guidance is obtained by using a new cost function that involves the integral of control energy divided by time-to-go to the nth power. This cost function was originally proposed by F. Reifler in an unpublished memorandum ("Primer of Optimal Control," Aug. 31, 1981). He derived a generalized form of proportional navigation using the new cost function. This guidance law drove the miss distance to zero but with no specification on final geometry. In Ref. 10 and the current paper, the GENEX law is derived using this same cost function, but with an additional constraint on final velocity orientation. This extends the previous work to allow explicit control of terminal geometry and is the main contribution of this paper.

The paper is organized as follows. In the next section, the linear optimal control problem is posed and solved in a general form. This is followed by its application to the familiar problem of proportional guidance. Then the new generalized form of explicit guidance containing a constraint on the terminal velocity vector is developed. A three-dimensional vector form of the guidance law is derived, and then its application to guidance in a single plane is used to illustrate the concept. This is followed by two application examples in which the guidance law performance is evaluated, first, for a missile versus air target scenario and, second, for an air-to-surface munition scenario. A brief summary of the paper is then presented.

II. Linear Optimal Control Problem

Define a set of linear state equations and boundary conditions as

$$\dot{\boldsymbol{X}} = A\boldsymbol{X} + \boldsymbol{b}u \quad \boldsymbol{X}(t_0) = \boldsymbol{X}_0 \quad \boldsymbol{X}(t_f) = \boldsymbol{X}_f = \boldsymbol{0} \tag{1}$$

where $\boldsymbol{X}$ is the state, u is the control, and $\boldsymbol{b}$ may be time-varying. The system of Eq. (1) is assumed to be fully controllable, with the control u unbounded. Select a cost function of the form

$$J = \int_0^{T_0} \frac{u^2}{2T^n}\,\mathrm{d}T = \int_0^{T_0} L(u, T)\,\mathrm{d}T \tag{2}$$

Received 6 December 2004; revision received 21 March 2005; accepted for publication 1 April 2005.

*Principal Aerospace Engineer, Engagement Systems Department, Attn: G82, 17320 Dahlgren Road. Associate Fellow AIAA.

†Senior Aerospace Engineer, Engagement Systems Department, Attn: G82, 17320 Dahlgren Road. Associate Fellow AIAA.

where $T = t_f - t$ is the time to go and n is an integer ≥ 0. Equation (2) is a generalization of the standard integral of control energy cost in which the inclusion of T^n in the denominator allows greater weight to be placed on the control usage as $T \to 0$. The effect becomes stronger as n becomes more positive. *Equation* (2) *thus comprises a family of cost functions parameterized by the index n. This is the sense in which explicit guidance is said to be generalized—by making the cost function dependant on the design parameter n.*

The *Hamiltonian* is defined by the scalar function

$$H = L + \boldsymbol{\lambda} \boldsymbol{f} \tag{3}$$

where $f = A\boldsymbol{X} + \boldsymbol{b}u$ and $\boldsymbol{\lambda} = \begin{bmatrix} \lambda_1 & \lambda_2 & \dots & \lambda_n \end{bmatrix}$ is a row vector.

The costate equations are

$$\dot{\boldsymbol{\lambda}} = -\frac{\partial H}{\partial \boldsymbol{X}} \tag{4}$$

The *minimum principle* of Pontryagin states that the control $\boldsymbol{u}$ is optimal when the Hamiltonian is minimized (see Ref. 13 for details). Thus, to find the optimal control $\boldsymbol{u}^*$, set

$$\frac{\partial H}{\partial \boldsymbol{u}} = 0 \tag{5}$$

The procedure is then to combine the state and costate equations to get $2n$ equations with $2n$ boundary conditions from which one can solve for $\boldsymbol{X}(t)$, $\boldsymbol{\lambda}(t)$, and $\boldsymbol{u}^*$.

Applying the minimum principle to the system of Eqs. (1) and (2) gives

$$L = \frac{u^2}{2T^n} \tag{6}$$

$$H = L + \boldsymbol{\lambda} \boldsymbol{f} = \frac{u^2}{2T^n} + \boldsymbol{\lambda}(A\boldsymbol{X} + \boldsymbol{b}u) \tag{7}$$

$$\frac{\mathrm{d}\boldsymbol{\lambda}}{\mathrm{d}T} = -\dot{\boldsymbol{\lambda}} = \frac{\partial H}{\partial \boldsymbol{X}} = \boldsymbol{\lambda} A \tag{8}$$

$$\frac{\partial H}{\partial u} = \frac{u}{T^n} + \boldsymbol{\lambda} \boldsymbol{b} = 0 \tag{9}$$

and

$$u^* = -\boldsymbol{\lambda} \boldsymbol{b} T^n \tag{10}$$

Now define a fundamental matrix $M(T)$ that satisfies

$$\frac{\mathrm{d}M}{\mathrm{d}T} = MA \quad M(T=0) = I \tag{11}$$

Equations (8) and (11) imply that

$$\boldsymbol{\lambda} = \boldsymbol{c} M \tag{12}$$

where $\boldsymbol{c}$ is a constant row vector. Then substitute Eq. (12) into (10) to obtain

$$u^* = -\boldsymbol{c} M \boldsymbol{b} T^n \tag{13}$$

The state equation may be rewritten as

$$\frac{\mathrm{d}\boldsymbol{X}}{\mathrm{d}T} = -A\boldsymbol{X} - \boldsymbol{b}u \tag{14}$$

Now consider the equation

$$\frac{\mathrm{d}(M\boldsymbol{X})}{\mathrm{d}T} = \frac{\mathrm{d}M}{\mathrm{d}T}\boldsymbol{X} + M\frac{\mathrm{d}\boldsymbol{X}}{\mathrm{d}T} \tag{15}$$

Substituting Eqs. (11) and (14) into (15) gives

$$\frac{\mathrm{d}(M\boldsymbol{X})}{\mathrm{d}T} = MA\boldsymbol{X} + M(-A\boldsymbol{X} - \boldsymbol{b}u) = -M\boldsymbol{b}u \tag{16}$$

In Eq. (13), because $\boldsymbol{c}$ is a row vector and $\boldsymbol{b}$ is a column vector, we have

$$\boldsymbol{c}M\boldsymbol{b} = (M\boldsymbol{b})^T \boldsymbol{c}^T = \text{scalar} \tag{17}$$

Thus

$$u^* = -(M\boldsymbol{b})^T \boldsymbol{c}^T T^n \tag{18}$$

Now substitute Eq. (18) into (16) and integrate:

$$\frac{\mathrm{d}(M\boldsymbol{X})}{\mathrm{d}T} = (M\boldsymbol{b})(M\boldsymbol{b})^T \boldsymbol{c}^T T^n \tag{19}$$

$$\int_0^T \mathrm{d}(M\boldsymbol{X}) = \left[\int_0^T (M\boldsymbol{b})(M\boldsymbol{b})^T T^n \,\mathrm{d}T\right] \boldsymbol{c}^T \tag{20}$$

because $\boldsymbol{c}$ is a constant vector.

Define the function

$$Q(T) = \int_0^T (M\boldsymbol{b})(M\boldsymbol{b})^T T^n \,\mathrm{d}T \tag{21}$$

Then Eq. (20) becomes

$$\int_0^T \mathrm{d}(M\boldsymbol{X}) = Q(T)\boldsymbol{c}^T \tag{22}$$

or, because $\boldsymbol{X} = \boldsymbol{0}$ at $T = 0$,

$$M\boldsymbol{X}(T) = Q(T)\boldsymbol{c}^T \tag{23}$$

Solving for $\boldsymbol{c}^T$ gives

$$\boldsymbol{c}^T = Q^{-1}(T)M(T)\boldsymbol{X}(T) = \text{constant} \tag{24}$$

and substituting Eq. (24) into (18) yields

$$u^* = -(M\boldsymbol{b})^T Q^{-1} M\boldsymbol{X} T^n \tag{25}$$

III. Results Applied to Proportional Navigation

To illustrate the application of these results, the case of proportional navigation guidance is considered. Let the lateral separation between a missile and its final point be

$$y = y_f - y_M \tag{26}$$

and define the *zero effort miss (ZEM)* as

$$z = y_f - y_M - \dot{y}_M T \tag{27}$$

Differentiating Eq. (27) gives

$$\dot{z} = -\dot{y}_M - \ddot{y}_M T - \dot{y}_M \dot{T} = -\ddot{y}_M T \tag{28}$$

because $\dot{T} = -1$. Let the control be missile acceleration and the state be the ZEM. Then the state equation is

$$\dot{X} = -uT, \qquad X(0) = X_0, \qquad X_f = 0 \tag{29}$$

This is of the form $\dot{\boldsymbol{X}} = A\boldsymbol{X} + \boldsymbol{b}u$ with $A = 0$ and $\boldsymbol{b} = -T$. From the definition of the fundamental matrix in Eq. (11), $M = I$. So

$$Q = \int_0^T T^{n+2} \,\mathrm{d}T = \frac{T^{n+3}}{n+3} \tag{30}$$

Substituting Eq. (30) into (25) gives

$$u^* = T[(n+3)/T^{n+3}]\boldsymbol{X}T^n = [(n+3)/T^2]\boldsymbol{X} \tag{31}$$

This is the proportional navigation acceleration command where $X = \text{ZEM}$ and the guidance gain is $\Lambda = n + 3$. A derivation of proportional navigation corresponding to Eq. (31) with $n = 0$ was given in Ref. 13, based on a specific linear–quadratic optimization.

IV. Generalized Vector Explicit Guidance

We now extend the previous results to include a *specification on the final velocity vector*. Let z be the zero effort miss with respect to a specified final position, and let v be the difference between current velocity and a desired final velocity. Define the states as

$$X_1 = z = y_f - y_M - \dot{y}_M T \tag{32a}$$

$$X_2 = v = \dot{y}_f - \dot{y}_M \tag{32b}$$

where

$$\dot{z} = -uT \tag{33a}$$

$$\dot{v} = -u \tag{33b}$$

subject to the terminal conditions $z = 0$ and $v = 0$ at $T = 0$.

The state equations may be written

$$\begin{bmatrix} \dot{z} \\ \dot{v} \end{bmatrix} = \begin{bmatrix} 0 & 0 \\ 0 & 0 \end{bmatrix} \begin{bmatrix} z \\ v \end{bmatrix} + \begin{bmatrix} -T \\ -1 \end{bmatrix} u \tag{34}$$

or

$$\dot{\boldsymbol{X}} = A\boldsymbol{X} + \boldsymbol{b}u, \qquad A = 0, \qquad \boldsymbol{b} = \begin{bmatrix} -T \\ -1 \end{bmatrix} \tag{35}$$

Since $A = 0$, we again have $M = I$, which gives

$$Q(T) = \int_0^T \boldsymbol{b}\boldsymbol{b}^T T^n \, \mathrm{d}T \tag{36}$$

Using

$$\boldsymbol{b}\boldsymbol{b}^T = \begin{bmatrix} T^2 & T \\ T & 1 \end{bmatrix} \tag{37}$$

we obtain

$$Q = \int_0^T \begin{bmatrix} T^{n+2} & T^{n+1} \\ T^{n+1} & T^n \end{bmatrix} \mathrm{d}T = \begin{bmatrix} \dfrac{T^{n+3}}{n+3} & \dfrac{T^{n+2}}{n+2} \\ \dfrac{T^{n+2}}{n+2} & \dfrac{T^{n+1}}{n+1} \end{bmatrix} \tag{38}$$

The inverse of Q may be obtained using

$$Q = \begin{bmatrix} a & b \\ c & d \end{bmatrix}, \qquad Q^{-1} = \frac{1}{D} \begin{bmatrix} d & -b \\ -c & a \end{bmatrix}, \qquad D = ad - bc \tag{39}$$

where

$$D = \left(\frac{T^{n+3}}{n+3}\right)\left(\frac{T^{n+1}}{n+1}\right) - \left(\frac{T^{n+2}}{n+2}\right)^2 = \frac{T^{2n+4}}{(n+1)(n+2)^2(n+3)} \tag{40}$$

Thus

$$Q^{-1} = \frac{(n+1)(n+2)^2(n+3)}{T^{2n+4}} \begin{bmatrix} \dfrac{T^{n+1}}{n+1} & -\dfrac{T^{n+2}}{n+2} \\ -\dfrac{T^{n+2}}{n+2} & \dfrac{T^{n+3}}{n+3} \end{bmatrix} \tag{41}$$

and

$$Q^{-1}T^n = \begin{bmatrix} (n+2)^2(n+3)T^{-3} & -(n+1)(n+2)(n+3)T^{-2} \\ -(n+1)(n+2)(n+3)T^{-2} & (n+1)(n+2)^2T^{-1} \end{bmatrix} \tag{42}$$

The optimum control is given by

$$u^* = -(M\boldsymbol{b})^T Q^{-1} M\boldsymbol{X}T^n = \begin{bmatrix} T & 1 \end{bmatrix} Q^{-1}T^n\boldsymbol{X} \tag{43}$$

Let

$$\begin{bmatrix} T & 1 \end{bmatrix} Q^{-1}T^n = \begin{bmatrix} C_1 & C_2 \end{bmatrix} \tag{44}$$

Then

$$u^* = \begin{bmatrix} C_1 & C_2 \end{bmatrix} \begin{bmatrix} z \\ v \end{bmatrix} = C_1 z + C_2 v \tag{45}$$

where

$$C_1 = (n+2)^2(n+3)T^{-2} - (n+1)(n+2)(n+3)T^{-2} \tag{46a}$$

$$C_2 = -(n+1)(n+2)(n+3)T^{-1} + (n+1)(n+2)^2T^{-1} \tag{46b}$$

Simplifying the above gives

$$C_1 = (n+2)(n+3)/T^2 \tag{47a}$$

$$C_2 = -(n+1)(n+2)/T \tag{47b}$$

Now define new gains:

$$K_1 = (n+2)(n+3) \tag{48a}$$

$$K_2 = -(n+1)(n+2) \tag{48b}$$

Then, combining Eqs. (45), (47), and (48) gives for the optimal control

$$u^* = 1/T^2 \left[K_1(y_f - y_M - \dot{y}_M T) + K_2(\dot{y}_f - \dot{y}_M)T\right] \tag{49}$$

For the case $n = 0$, the guidance gains become $K_1 = 6$, $K_2 = -2$.

The choice of n may be determined by parameter optimization studies that specify additional performance objectives and constraints on the missile. In general, n may be used to modify the curvature of the trajectory, while enforcing a specified final position and velocity orientation.

A physical interpretation of the optimal control in Eq. (49) is as follows: The control consists of two terms, the first a proportional-navigation–like term proportional to the zero effort miss, and the second term proportional to the difference between current and desired final velocity. The first term drives the collision course heading error to zero, and the second term enforces a specification on the final velocity vector orientation.

In implementing the GENEX law, it is important to note that the acceleration command u is continually updated during guidance, based on improved estimates of predicted intercept point, missile states, ZEM, and time-to-go.

V. Vector Form of Explicit Guidance

Assuming Eq. (49) has a similar form in the x and z coordinates, a vector form of the guidance law may be written as

$$\boldsymbol{u} = 1/T^2[K_1(\boldsymbol{R}_f - \boldsymbol{R}_M - \boldsymbol{V}_M T) + K_2(\boldsymbol{V}_f - \boldsymbol{V}_M)T] \tag{50}$$

Now let

$$\boldsymbol{R}_f - \boldsymbol{R}_M = R\hat{r}, \qquad \boldsymbol{V}_M = V\hat{v}, \qquad \boldsymbol{V}_f = V\hat{v}_f, \qquad T = R/V \tag{51}$$

where R is range to go, V is average remaining missile speed, and $\hat{r}$, $\hat{v}$, and $\hat{v}_f$ are unit vectors along $\boldsymbol{R}$, $\boldsymbol{V}_M$, and $\boldsymbol{V}_f$, respectively. Because the missile is guided to a predicted intercept point, V also represents the average closing speed to that point. In some applications, a special algorithm is employed to estimate the average remaining speed. However, in practice, it often suffices to replace V with the current missile speed V_M. This approximation can work well because the estimate of speed is continually updated throughout the flight.

Substituting Eq. (51) into (50) gives

$$\boldsymbol{u} = 1/T^2[K_1(R\hat{r} - VT\hat{v}) + K_2VT(\hat{v}_f - \hat{v})] \tag{52}$$

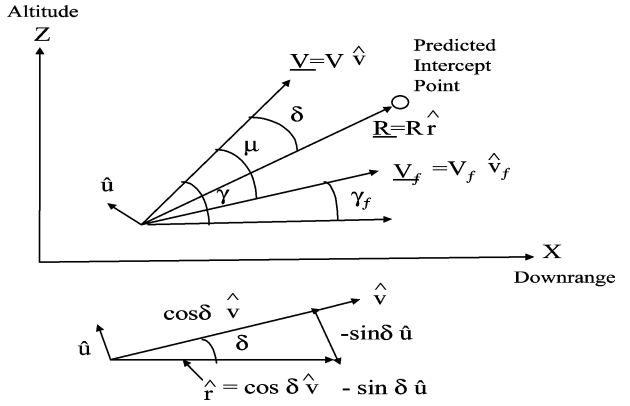

Fig. 1 Geometry for planar guidance example.

Because $VT = R$, we also have

$$\boldsymbol{u} = V^2/R[K_1(\hat{r} - \hat{v}) + K_2(\hat{v}_f - \hat{v})] \tag{53}$$

For a vehicle with no longitudinal control capability, not all of the above is controllable. It may be shown that the component of $\boldsymbol{u}$ normal to the velocity vector in Eq. (53) is given by

$$\boldsymbol{u}_\perp = V^2/R[K_1(\hat{r} - \hat{v}\cos\delta) + K_2(\hat{v}_f - \hat{v}\cos\mu)] \tag{54}$$

where the heading error δ and the velocity error μ are defined by

$$\cos\delta = \hat{r}\cdot\hat{v}, \qquad \cos\mu = \hat{v}_f\cdot\hat{v} \tag{55}$$

VI. Illustration of Guidance Law in a Single Plane

One may examine the above for the case of guidance in a single plane. Consider the diagrams in Fig. 1.

Let $\hat{u}$ denote a unit vector normal to $\hat{v}$ in the direction of the normal acceleration $\boldsymbol{u}$. Referring to the lower sketch in Fig. 1, we may write each of the unit vectors $\hat{r}$ and $\hat{v}_f$ as the vector sum of a projection along $\hat{v}$ and a component normal to $\hat{v}$:

$$\hat{r} = \hat{v}\cos\delta - \hat{u}\sin\delta, \qquad \hat{v}_f = \hat{v}\cos\mu - \hat{u}\sin\mu \tag{56}$$

where $\mu = \gamma - \gamma_f$. If the above are substituted into (54) there results

$$\boldsymbol{u} = V^2/R[-K_1\sin\delta - K_2\sin(\gamma - \gamma_f)]\hat{u} \tag{57}$$

Thus, the guidance law consists of a term proportional to the heading error (δ) and a term proportional to the difference between current and desired final flight path angle (μ).

VII. Example: Terminal Guidance vs Maneuvering Target

To illustrate the application of GENEX guidance, results were generated for a missile–target engagement scenario under the assumption of perfect information about the target and missile states. For this scenario, the target was performing an evasive maneuver, and the missile had a first-order lag in its response to acceleration commands. The conditions defining the engagement are provided in Table 1.

In the engagement, the target and missile are closing, with an initial separation of 5000 m. The missile is launched 500 m above the target with an initial azimuth heading angle of −10 deg. The target has an initial horizontal heading angle of +18.4 deg (i.e., in a direction opposite to the missile). In addition, the target pulls a 3-g maneuver starting at time zero, again in a direction opposite to the initial missile heading.

The missile and target trajectories in the vertical and horizontal planes are shown in Fig. 2. The missile pulls down from above the target and executes a horizontal maneuver to intercept the target. Besides reducing the miss distance to a small value, the missile is required to arrive at the intercept with a zero degree relative crossing

Table 1 Assumed conditions for engagement scenario

Parameter	Assumed value
Initial horizontal separation, R_o	5000 m
Initial vertical separation, $h_M - h_T$	500 m
Missile speed, V_M	600 m/s
Target speed, V_T	316 m/s
Time of flight, T_0	6.2 s
Maximum missile acceleration, $A_{\max}$	50 g
Target acceleration, A_T	3 g
Missile initial heading angle, ψ_M	−10 deg
Target initial heading angle, ψ_T	18.4 deg
Missile time constant, τ	0.1 s
GENEX guidance design parameter, n	1
Specified terminal crossing angle, $\cos^{-1}(-\hat{x}_M\cdot\hat{x}_T)$	0 deg (head on)

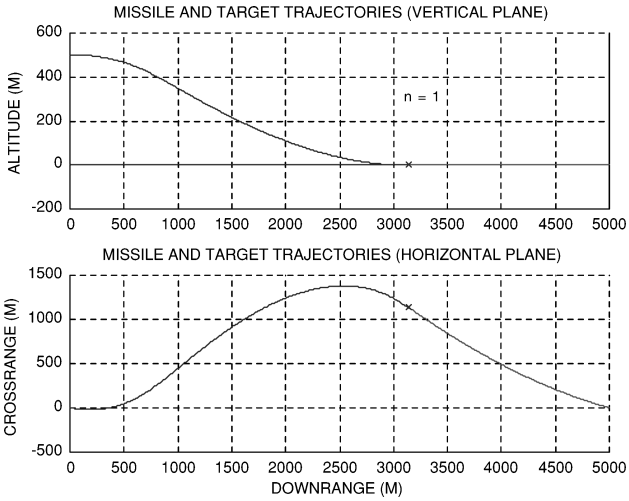

Fig. 2 Missile and target trajectories.

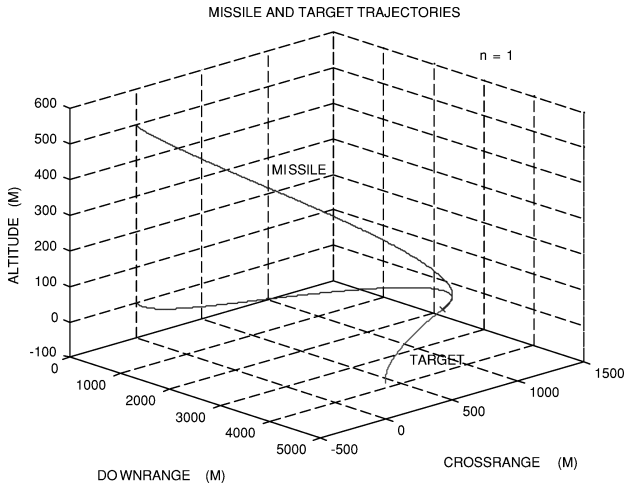

Fig. 3 Three-dimensional view of engagement.

angle between the missile and target velocity vectors. The results of Fig. 2 show that both objectives are accomplished. A final miss distance of 0.04 m is achieved while the crossing angle is 0.18 deg. To achieve this aspect in a nose on encounter, the missile must maneuver to lead the target, and then reverse its path to turn back into the target. The GENEX design parameter used for this example was $n = 1$.

Figure 3 shows the engagement in a 3-dimensional view. The curving path of the missile as it descends and bends around to achieve a zero aspect is clearly illustrated. In Fig. 4, the histories of the commanded and achieved accelerations of the missile and the horizontal and vertical flight path angles are illustrated. The

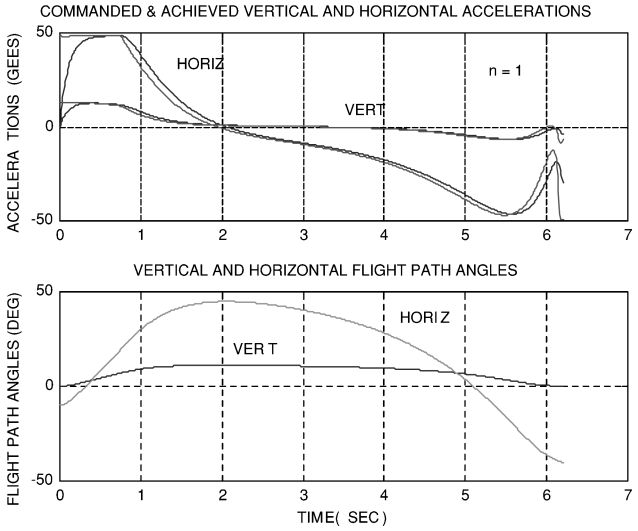

Fig. 4 Acceleration and flight-path angle histories.

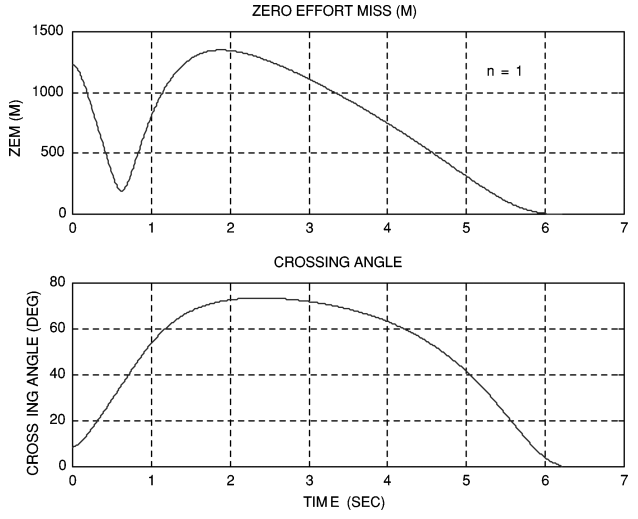

Fig. 5 Zero-effort miss and crossing angle histories.

horizontal component of missile acceleration initially saturates, but later recovers in time to close out the miss distance and relative heading error. Figure 5 shows the time histories of the zero-effort miss and the relative crossing angle. The ZEM is computed based on target and missile velocities, but not including the effects of acceleration. Near the end of the engagement, both the ZEM and the crossing angle approach the desired value of zero.

The effect of varying the GENEX design parameter is illustrated in Figs. 6 through 8 for values of $n = 0$, 1, and 2. These figures clearly illustrate how the value of n influences the curvature of the trajectory. As n is increased, the missile's trajectory exhibits more aggressive curvature in converging to the final crossing angle. Note, for example, in Fig. 8 that for $n = 0$, the missile does not achieve the desired 0-deg crossing angle, whereas for $n = 1, 2$ it does. However, higher values of n come at the expense of higher called-for accelerations and allow the possibility of saturation, which may prevent intercepting the target or achieving the desired terminal conditions.

As in any homing problem, the ability to achieve specified crossing angles at intercept together with a small miss will obviously depend on the available homing time, the relative acceleration advantage of the missile with respect to the target, missile response lag, and guidance gain. For some scenarios these conditions may not allow certain final crossing angles and/or small miss to be achieved. In addition, the effect of sensor errors and noise, and imprecise estimation of target states (particularly target acceleration), will reduce

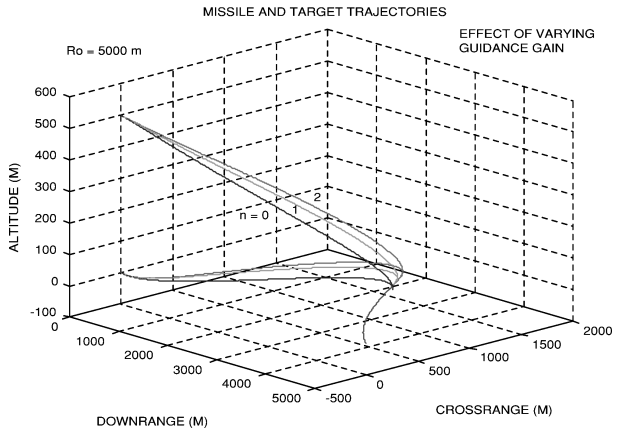

Fig. 6 Three-dimensional view of engagement: effect of design parameter *n*.

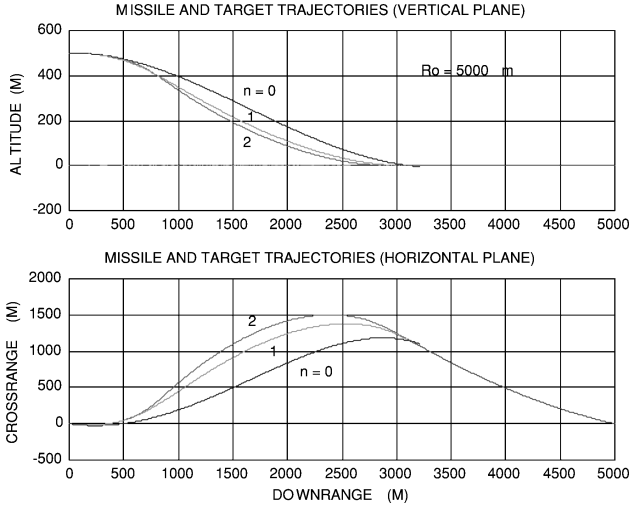

Fig. 7 Missile and target trajectories: effect of design parameter *n*.

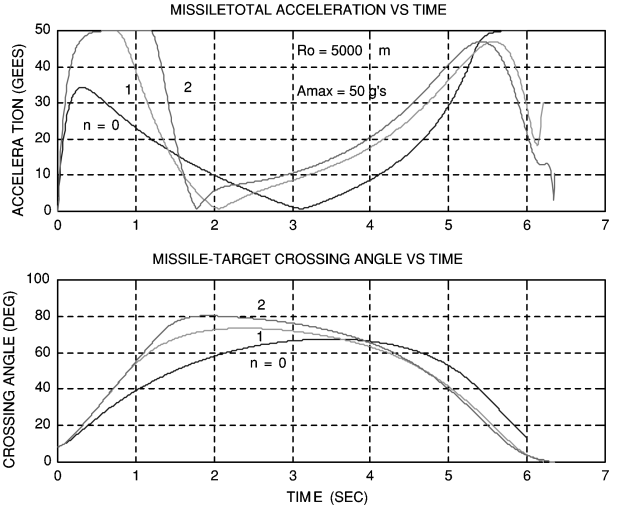

Fig. 8 Acceleration and crossing angle histories: effect of design parameter *n*.

terminal homing performance, and must be examined in detail using statistical Monte Carlo analysis with a full suite of system errors.

VIII. Example: Guidance for a Weaponized UAV Munition

The GENEX guidance algorithm was used to investigate trajectory and guidance design for a small, gliding, inertially-navigated, air-to-surface munition that is released from a weaponized

unmanned aerial vehicle (UAV). The UAV flies at a subsonic speed and releases the munition in level flight with a negligible downward ejection velocity. The UAV contains a sensor that acquires the target and determines its position based on the UAV navigation solution and the measured range and line-of-sight angle to the target. The estimated target location is used as the aimpoint for the munition. Release of the munition may be delayed based on the feasible target engagement region (relative to the release point) and other mission objectives. Prior to release, the navigation solution and the aimpoint are transferred to the munition's guidance, navigation, and control (GNC) unit. The munition does not contain a seeker and the aimpoint is not updated during the flight. A typical mission is shown in Fig. 9.

The munition's airframe is shown in Fig. 10. The rear section is the GNC unit with active tail fins for control, and the midsection consists of a blast fragmentation warhead. The forward section contains a heavy penetrator nose with four fixed canards molded into a lightweight nose cap. Because the total lifting surface area is small, the maneuverability of the munition is limited. At a speed of 800 ft/s, the maximum trimmed angle of attack is 21 deg, corresponding to a maximum normal force coefficient, C_N, of 3.5. Assuming a weight of 75 lb and a body diameter of 5 in., the munition's maximum maneuverability is about 5 g. The destabilizing influence of the fixed canards allows the airframe to achieve a 0.5-s time constant with only a few degrees of fin deflection.

The desire to maximize the effectiveness of the warhead and the survivability of the UAV drives the selection of its cruise altitude. This, in turn, places constraints on the munition trajectory design. Ensuring warhead effectiveness requires, in addition to a small miss, that the final flight path angle at impact be steeper than 85 deg. To increase survivability of the UAV, it is desired to keep its altitude as low as possible but above a 1000-ft minimum limit to provide a clear line of sight to the target over various terrains. Additionally, it is necessary to achieve the final vertical flight-path angle within the acquisition range of the UAV sensor. With a 3-n mile acquisition range, and release altitudes less than 5000 ft, it is difficult to achieve the desired terminal angle because of the limited maneuverability.

The GENEX guidance law was used to design munition trajectories satisfying the miss distance and terminal angle constraints. Figure 11 shows results for a 5000-ft altitude release against a 3-n mile downrange aimpoint. Three trajectories are shown with three different values of the design parameter n. For this release condition, the desired final flight-path angle could only be achieved with values of $n = 1$ and 2.

Figure 12 shows trajectories to an aimpoint at 3 n miles downrange for a 3000-ft release altitude. As before, values of n greater than or equal to one were necessary to achieve the required final flight path angle. Regardless of the value of n, the desired angle could not be achieved for release altitudes below 3000 ft. Terminal conditions for release altitudes of 5000, 4000, and 3000 ft are given in Table 2.

The effect of the design parameter on acceleration limiting was examined for a 3000-ft release scenario. The acceleration command was limited to a value corresponding to the maximum angle of attack. The $n = 0$ guidance had lower acceleration commands early in the flight and the trajectory took a more direct path toward the aimpoint. The $n = 1$ and 2 trajectories were acceleration-command-limited initially with the $n = 2$ trajectory, riding the limit for a longer time. Near the end of the flight, all three guidance laws saturated as the time-to-go approached zero. The $n = 0$ trajectory failed to achieve the desired final flight path angle.

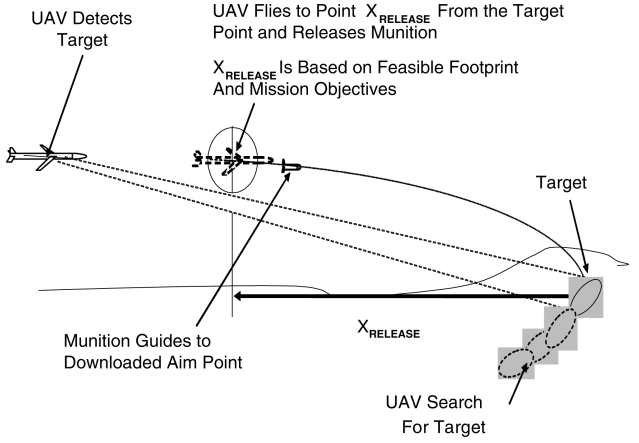

Fig. 9 Weaponized UAV mission.

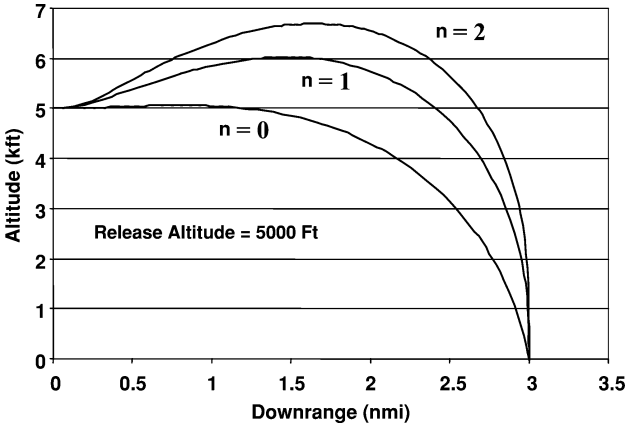

Fig. 11 5000-ft release.

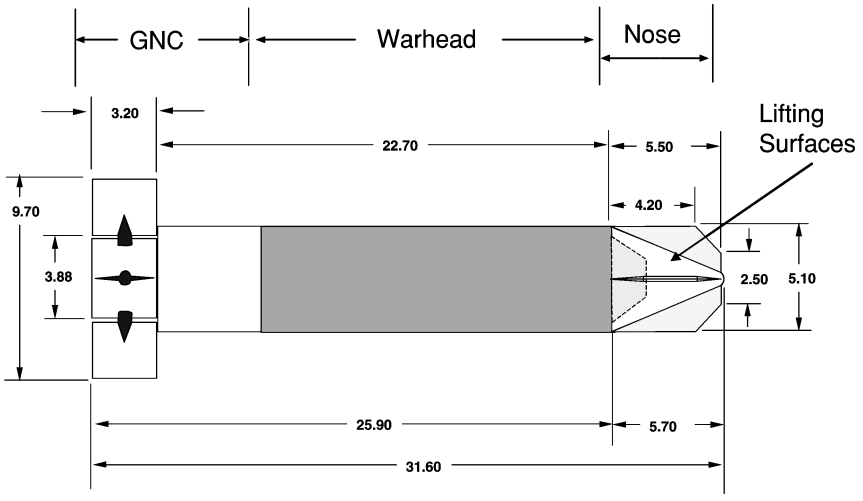

Fig. 10 Munition Airframe.

Table 2 Terminal conditions for three release altitudes

	5000-ft release			4000-ft release			3000-ft release		
Design parameter n	0	1	2	0	1	2	0	1	2
Flight time, s	28.3	34.8	41.6	28.9	37.0	46.3	28.5	37.9	50.3
Final speed, ft/s	678.	612.	631.	649.	562.	578.	622.	535.	474.
Final flight-path angle, deg	82.7	89.3	89.8	66.3	87.8	89.8	61.4	87.4	88.0

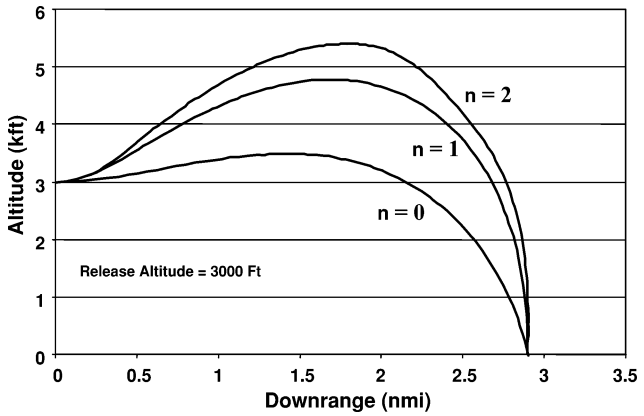

Fig. 12 3000-ft release.

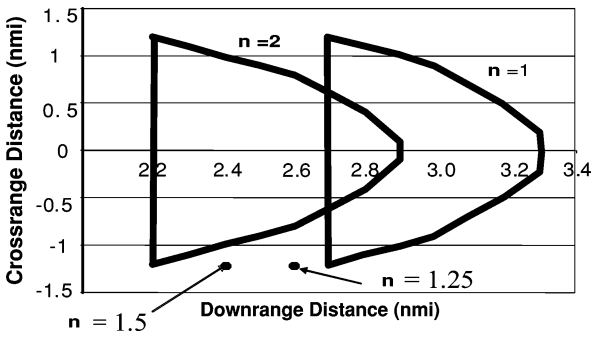

Fig. 13 Feasible engagement zones.

An important metric for the guidance design is the set of target locations that can be engaged for a specified munition release point. Should a target be detected closer to the UAV than the minimum range boundary, the target would be engaged by a flyback of the UAV to place the target within the munition's lethal footprint. The time required for the UAV to complete this maneuver can be appreciable and thus can lead to an undesirable delay in target destruction. So maximizing the feasible target engagement region is highly desirable in order to minimize the response time of the weapon for engaging a target.

Figure 13 shows the target engagement regions that can be achieved using GENEX with $n = 1$ and 2. For these values, each region shows the target range/crossrange points at which the final flight angle may be achieved. The smaller value of n allows the required final flight-path angle to be achieved at longer ranges. Figure 13 also shows two outlying points that were successfully engaged using intermediate (noninteger) parameter values. It was found that the gaps between the two regions in Fig. 13 could be filled in using intermediate values of n between 1 and 2. In the design of the guidance algorithm, the parameter n would be scheduled as a function of the downrange and crossrange positions of the target relative to the current release point.

The GENEX guidance algorithm provided a valuable tool for maximizing the target engagement region for the guided air-to-surface munition with a vertical final flight-path angle constraint. Guidance design parameters between 1 and 2 were adequate in meeting the terminal trajectory constraints. Values greater than 2 produce little additional benefit and values less than 1 were unable to satisfy the terminal constraint.

IX. Conclusions

This paper has derived and evaluated the performance of a generalized form of explicit guidance. The generalized vector explicit guidance (GENEX) law has the ability to achieve design specifications on miss distance and final missile-target relative orientation simultaneously. The latter specification may be used to enhance the performance of warheads the effectiveness of which is influenced by the terminal encounter geometry. The GENEX guidance law is parameterized in terms of a design coefficient that is specified by the user and which determines the degree of curvature (and hence control usage) in the trajectory.

Feasibility of the GENEX guidance law was demonstrated by its application to two weapon scenarios. In the first, a missile terminal homing scenario, the guidance was shown to perform well against an air target performing evasive maneuvers. The specified zero aspect terminal encounter angle was achieved while simultaneously minimizing miss distance. The analysis assumed ideal sensor information, and a simplified single-lag missile response model. In the second case, an air-to-surface munition released from an unmanned air vehicle was evaluated in terms of its ability to achieve a nearly vertical final impact angle. In addition, it was desired to maximize the size of the surface target engagement region. The GENEX guidance law was able to produce trajectories satisfying the terminal angle constraint. An engagement region of sufficient size was shown to be achievable using design parameters between 1 and 2, which were scheduled as a function of target location and weapon release altitude.

Results of these studies are preliminary. More detailed analyses would need to consider higher fidelity weapon models incorporating six-degree-of-freedom dynamics, nonlinear and coupled aerodynamics, and detailed autopilot descriptions. A target state estimator and complete sensor noise model would also need to be included. The models should then be exercised over a greater range of scenarios to more fully evaluate the performance of the guidance law in a realistic setting.

References

[1]Cherry, G., "A General Explicit, Optimizing Guidance Law for Rocket-Propelled Spacecraft," AIAA Paper 64-638, Aug. 1964.

[2]Lin, C. F., *Modern Navigation, Guidance, and Control Processing*, Prentice–Hall, Englewood Cliffs, NJ, 1991, Sec. 8.6.

[3]Zarchan, P., *Tactical and Strategic Missile Guidance, 4th ed.*, Progress in Astronautics and Aeronautics, Vol. 199, AIAA, Reston, VA, 2002, Chap. 25.

[4]Kim, M., and Grider, K. V., "Terminal Guidance for Impact Attitude Angle Constrained Flight Trajectories," *IEEE Transactions on Aerospace and Electronic Systems*, Vol. 9, No. 6, 1973, pp. 852–859.

[5]Kim, B. S., Lee, G. L., and Han, H. S., "Biased PNG Law for Impact with Angular Constraint," *IEEE Transactions on Aerospace and Electronic Systems*, Vol. 34, No. 1, 1998, pp. 277–288.

[6]Song, T. L., and Shin, J. S., "Time Optimal Impact Angle Control for Vertical Plane Engagements," *IEEE Transactions on Aerospace and Electronic Systems*, Vol. 35, No. 2, 1999, pp. 738–742.

[7]Song, T. L., Shin, J. S., and Han, H. S., "Impact Angle Control for Planar Engagements," *IEEE Transactions on Aerospace and Electronic Systems*, Vol. 35, No. 4, 1999, pp. 1439–1444.

[8]Menon, P. K., and Ohlmeyer, E. J., "Integrated Guidance-Control Systems for Fixed-Aim Warhead Missiles," ADA386510, URL: http://www.optisyn.com/research/papers/papers/2000/MSCd2000.pdf [cited 7 Nov. 2000].

[9]Manchester, I. R., and Savkin, A. V., "Circular Navigation Guidance Law for Precision Missile Target Engagements," *Proceedings of the 41st IEEE Conference on Decision and Control*, Vol. 2, Institute of Electrical and Electronics Engineers, Piscataway, NJ, 2002, pp. 1287–1292.

[10]Ohlmeyer, E. J., "Control of Terminal Engagement Geometry Using Generalized Vector Explicit Guidance," *Proceedings of American Control Conference*, Vol. 1, Institute of Electrical and Electronics Engineers, Piscataway, NJ, 2003, pp. 396–401.

[11]Savkin, A. V., Pathirana, P., and Faruqi, F. A., "The Problem of Precision Missile Guidance: LQR and H∞ Frameworks," *IEEE Transactions on Aerospace and Electronic Systems*, Vol. 39, No. 3, 2003, pp. 901–910.

[12]Manchester, I. R., and Savkin, A. V., "Circular Navigation Missile Guidance with Incomplete Information and Uncertain Autopilot Model," *Journal of Guidance, Control and Dynamics*, Vol. 27, No. 6, 2004, pp. 1078–1083.

[13]Bryson, A. E., and Ho, Y.-C., *Applied Optimal Control*, Blaisdell, Waltham, MA, 1969.